arXiv:1507.06742v2 [nucl-th] 11 Aug 2015

Constraining heavy quark energy loss using B and D meson measurements in heavy ion collision at RHIC and LHC energies

Kapil Saraswat[a], Prashant Shukla[b,c,*], Venktesh Singh[a]

[a] *Department of Physics, Banaras Hindu University, Varanasi 221005, India.*
[b] *Nuclear Physics Division, Bhabha Atomic Research Centre, Mumbai 400085, India.*
[c] *Homi Bhabha National Institute, Anushakti Nagar, Mumbai 400094, India.*

Abstract

In this work, we calculate energy loss of heavy quark (charm and bottom) due to elastic collisions and gluon radiation in hot/dense medium. The collisional energy loss has been obtained using QCD calculations. The radiative energy loss is calculated using reaction operator formalism and generalized dead cone approach. We rederive the energy loss expression using same assumptions as generalized dead cone approach but obtain slightly different results. We also improve the model employed to calculate path length and the system evolution. The nuclear modification factors R_{AA} including shadowing and energy loss are evaluated for B and D mesons and are compared with the measurements in PbPb collision at $\sqrt{s_{NN}} = 2.76$ TeV and with the D meson and Heavy flavour (HF) electrons measurements in AuAu collision at $\sqrt{s_{NN}} = 200$ GeV. The radiative energy loss calculated by reaction operator formalism added with collisional energy loss describes the RHIC HF electron suppression in high p_T range. It also describes the LHC measurement of B meson suppression but overestimates the suppression of D meson. The radiative energy loss from generalized dead cone approach describes the charm suppression at both RHIC as well as LHC energies and requires energy loss due to collisions to be added in order to describe the bottom suppression at LHC.

*Corresponding author
Email address: pshukla@barc.gov.in (Prashant Shukla)

Keywords: QGP, heavy quark energy loss, radiative and collisional energy loss

1. Introduction

The heavy ion collisions at ultra relativistic energy create matter with high energy density required to form Quark Gluon Plasma (QGP). Relativistic Heavy Ion Collider (RHIC) and Large Hadron Collider (LHC) are designed to create and explore QGP. Many measurements at RHIC and LHC already point to the formation of QGP [1]. The heavy quarks (charm and bottom) are produced in hard partonic interactions in heavy ion collisions and their initial momentum distribution can be calculated from pQCD [2]. While traversing the hot/dense medium formed in the collisions, these quarks loose energy either due to the elastic collisions with the plasma constituents or by radiating a gluon or both. There are several formulations to calculate collisional [3, 4, 5, 6, 7] as well as radiative energy loss [8, 9, 10, 11]. For a review of many of these formalism see Ref. [12]. At high parton energies, the radiative energy loss becomes much larger than the collisional energy loss but at lower energies, these two processes can contribute equally with the collisional energy loss being the dominant for small values of the parton energy [13].

There are many heavy quark energy loss models, each having specific set of simplifications/assumptions. The model by Gyulassy, Levai and Vitev (GLV) [14, 15] is based on a systematic expansion of the energy loss in terms of the number of scatterings and generally leading order term is included in the current calculations. The medium is characterized by two parameters, the density of scattering centers or mean free path and Debye screening mass. Such an approach includes the interference between vacuum and medium induced radiation. This formalism was then extended to obtain the energy loss for heavy quarks in Ref. [11] and was simplified for the first order of opacity expansion in Ref. [16]

In this work, we calculate the radiative energy loss of heavy quarks (both charm or bottom quark) using reaction operator formalism DGLV (Djordjevic, Gyulassy, Levai and Vitev) [10, 11, 16] and using generalized dead cone approach AJMS (Abir, Jamil, Mustafa and Srivastava) [17]. We rederive the energy loss expression using same assumptions as generalized dead cone approach but obtain slightly different results. We also improve the model employed to calculate path length and the system evolution. The collisional energy loss has been calculated using Peigne and Peshier formalism [7]. The nuclear modification factors R_{AA} including shadowing and energy loss are evaluated for B and D mesons and are compared with the measurements in PbPb collision at $\sqrt{s_{NN}} = 2.76$ TeV and with the HF electron measurement of PHENIX and D meson measurements of STAR in AuAu collision at $\sqrt{s_{NN}} = 200$ GeV.

2. Heavy Quark Production by Hard Processes

The production cross sections of $c\bar{c}$ and $b\bar{b}$ pairs are calculated to NLO in pQCD using the CT10 parton densities [18]. We use the same set of parameters as that of Ref. [19] which are obtained by fitting the energy dependence of open heavy flavor production to the measured total cross sections. The charm quark mass and scale parameters used are $m_c = 1.27$ GeV, $\mu_F/m_{T\,c} = 2.10$, and $\mu_R/m_{T\,c} = 1.60$ [19]. The bottom quark mass and scale parameters are $m_b = 4.65$ GeV, $\mu_F/m_{T\,b} = 1.40$, and $\mu_R/m_{T\,b} = 1.10$. Here μ_F is the factorization scale, μ_R is the renormalization scale and $m_T = \sqrt{M^2 + p_T^2}$. The central EPS09 NLO parameter set [20] is used to calculate the modifications of the parton distribution functions (nPDF) in heavy ion collisions, referred as shadowing effects.

For the fragmentation of heavy quarks into mesons, Peterson fragmentation function is used which is given as follows [21]

$$D_Q(z) = \frac{N}{z[1 - (1/z) - \epsilon_Q/(1-z)]^2}. \tag{1}$$

Here $z = p_T^D/p_T^c$ and N is normalization constant which is fixed by summing

over all hadrons containing heavy quark,

$$\sum \int dz D_Q(z) = 1. \tag{2}$$

We take $\epsilon_c = 0.016$ and $\epsilon_b = 0.0012$. The schemes of D meson to electron decay (BR = 10.3 %) and B meson to J/ψ decay (BR = 1.1 %) are obtained by Pythia simulations [22].

Figure 1 shows the NLO calculations of differential cross section of single electrons from D mesons as a function of the transverse momentum p_T in pp collision at $\sqrt{s} = 200$ GeV compared with the PHENIX measurements of single electrons from heavy flavour [23]. As shown in the Data/Theory panel the agreement between the data and the calculations is not very good but since at p_T above 2 GeV/c the shapes of the calculations and the data are same, it does not affect the R_{AA} calculations due to energy loss.

Figure 2 shows the NLO calculations of differential cross section of D^0 mesons as a function of the transverse momentum p_T in pp collision at $\sqrt{s} = 2.76$ TeV compared with ALICE measurements of D^0 and D^+ mesons [24]. Here also Data/Theory panel shows the agreement between the data and the calculations is not very good but since at p_T above 2 GeV/c the shapes of the calculations and the data are same, it does not affect the R_{AA} calculations due to energy loss.

Figure 3 shows the NLO calculations of differential cross section of inclusive J/ψ coming from B mesons as a function of the transverse momentum p_T in pp collision at $\sqrt{s} = 2.76$ TeV.

3. Collisional Energy Loss

The QCD calculation of the rate of energy loss of heavy quark per unit distance (dE/dx) in QGP is given by Braaten and Thoma [4]. Their formalism is an extension of QED calculation of dE/dx for a muon [6] which assumes that the momentum exchange $q \ll E$. Such an assumption is not valid in the domain

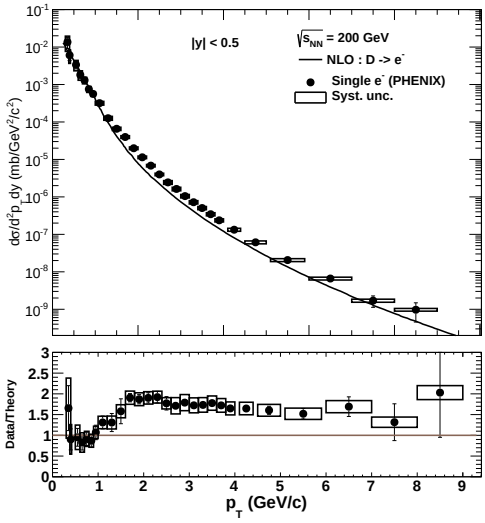


Figure 1: (color online): The NLO calculations of differential cross section of single electrons from D mesons as a function of the transverse momentum p_T in pp collision at $\sqrt{s} = 200$ GeV. The data is from PHENIX measurements of single electrons from heavy flavour [23].

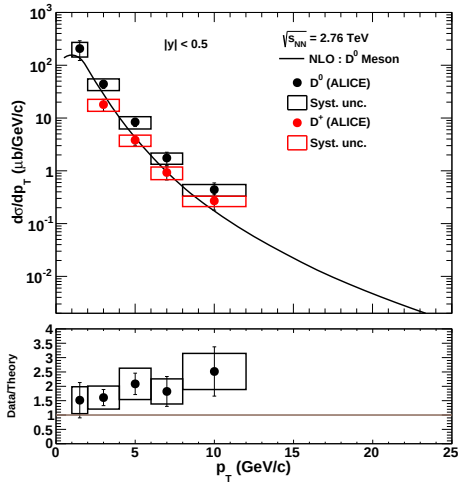


Figure 2: (color online): The NLO calculations of differential cross section of D^0 mesons as a function of the transverse momentum p_T in pp collision at $\sqrt{s} = 2.76$ TeV. The data is from ALICE measurements of D^0 and D^+ mesons [24].

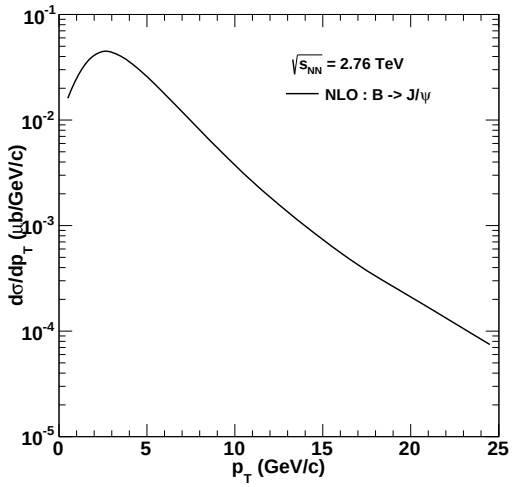


Figure 3: (color online): The NLO calculations of differential cross section of inclusive J/ψ coming from B mesons as a function of the transverse momentum p_T in pp collision at $\sqrt{s} =$ 2.76 TeV.

when the energy of the heavy quark $E \gg M^2/T$, where M is the mass of the heavy quark. Peigne and Peshier (PP) [7] extended this calculation which is valid in the domain $E \gg M^2/T$ to give the expression for dE/dx as

$$\frac{dE}{dx} = \frac{4\pi\alpha_s^2 T^2}{3}\left[\left(1+\frac{N_f}{6}\right)\log\left(\frac{ET}{\mu_g^2}\right)+\frac{2}{9}\log\frac{ET}{M^2}+c(N_f)\right]. \qquad (3)$$

Here $\mu_g = \sqrt{4\pi\alpha_s T^2\left(1+N_f/6\right)}$ is the Debye screening mass and $c(N_f) \approx 0.146N_f + 0.05$. $\alpha_s(= 0.3)$ is the fine structure splitting constant for strong interaction and N_f is the number of quark flavours.

4. Radiative Energy Loss

4.1. DGLV Formalism

The energy loss of fast partons is dominated by radiation of gluons. The reaction operator formalism is used in Ref. [10] to obtain the energy loss due to gluon radiation for light quark jets. Analytical expression is obtained for energy loss in

powers of gluon opacity (L/λ) where λ is the mean free path of the quark and L is the path length traversed in the medium. This formalism was then extended to obtain the energy loss for heavy quarks in Ref. [11] and was simplified for the first order of opacity expansion in Ref. [16]. The expression of the average radiative energy loss of heavy quark is given in appendix **A**.

4.2. Generalized Dead Cone Approach (AJMS)

The rate of radiative energy loss of a heavy quark with energy E due to the inelastic scattering with the medium is calculated as

$$\frac{dE}{dx} = \frac{<\omega>}{\lambda}, \tag{4}$$

where $<\omega>$ is the mean energy of the emitted gluons.
The probability of gluon emission off a heavy quark is written as [17]

$$\frac{d\eta_g}{d\eta\ d\omega} = \frac{2C_A\alpha_s}{\pi}\ \frac{\mathcal{D}}{\omega}\ \ , \tag{5}$$

where $C_A(=3)$ is the Casimir operator in QCD and ω is related to the transverse momentum of the emitted gluons $k_\perp$ by the relation $k_\perp = \omega\ \sin\theta$, where θ is the emission angle. $\mathcal{D}$ is the generalised dead cone which can be written as [25]

$$\mathcal{D} = \left(1 + \frac{M^2}{s}\ e^{2\eta}\right)^{-2}\ \ ,\ \eta = -\ln\tan\left(\frac{\theta}{2}\right)\ \ . \tag{6}$$

Here s is mandelstam variable which is related to the energy E and mass M of heavy quark by the relation, $s = 2E^2 + 2E\sqrt{E^2 - M^2} - M^2$.

The mean energy of the emitted gluon can be written as [17]

$$<\omega> = \frac{\int \frac{d\eta_g}{d\eta d\omega}\ \omega\ d\eta\ d\omega}{\int \frac{d\eta_g}{d\eta d\omega}\ d\eta\ d\omega}\ =\ \frac{\int d\omega\ \int\ \mathcal{D}\ d\eta}{\int \frac{1}{\omega}\ d\omega\ \int \mathcal{D}\ d\eta}\ \ . \tag{7}$$

The mean free path length λ is calculated as [17]

$$\frac{1}{\lambda} = \rho_q\ \sigma_{Qq(\bar{q})\to Qq(\bar{q})g} + \rho_g\ \sigma_{Qg\to Qgg}\ , \tag{8}$$

$$= (\rho_q + \frac{9}{4}\ \rho_g)\ \sigma_{2\to 3}, \tag{9}$$

$$= \rho_{QGP}\ \sigma_{2\to 3}\ . \tag{10}$$

The total cross section of the process $2 \to 3$ is calculated as [26]

$$\sigma_{2\to3} = 4\ C_A\ \alpha_s^3\ \int\ \frac{1}{(q_\perp^2)^2}\ dq_\perp^2\ \int\ \frac{1}{\omega}\ d\omega\ \int\ \mathcal{D}\ d\eta\ \ . \tag{11}$$

Here $q_\perp$ is the transverse momentum of the exchanged gluon. Using Eqs. (4), (7), (8) and (11) and assigning the limits of the variables of q^2, ω and η we get

$$\frac{dE}{dx} = 24\ \alpha_s^3\ \rho_{QGP}\ \int_{q_\perp^2|_{min}}^{q_\perp^2|_{max}}\ \frac{1}{(q_\perp^2)^2}\ dq_\perp^2\ \int_{\omega_{min}}^{\omega_{max}}\ d\omega\ \ \int_{\eta_{min}}^{\eta_{max}}\ \mathcal{D}\ d\eta\ \ . \tag{12}$$

Here we have put C_A=3 and factor of 2 is used to cover both upper and lower hemispheres of η.

Equation (12) is solved to get following result (see details in appendix **B**) which we call corrected AJMS result

$$\frac{dE}{dx} = 24\ \alpha_s^3\ \rho_{QGP}\ \frac{1}{\mu_g}\ \Big(1-\beta_1\Big)\ \left(\sqrt{\frac{1}{(1-\beta_1)}\ \log\Big(\frac{1}{\beta_1}\Big)} - 1\right)\ \mathcal{F}(\delta)\ \ . \tag{13}$$

Here

$$\mathcal{F}(\delta) = 2\delta - \frac{1}{2}\ \log\left(\frac{1+\frac{M^2}{s}\ e^{2\delta}}{1+\frac{M^2}{s}\ e^{-2\delta}}\right) - \left(\frac{\frac{M^2}{s}\ \sinh(2\delta)}{1+2\ \frac{M^2}{s}\cosh(2\delta)+\frac{M^4}{s^2}}\right)\ \ . \tag{14}$$

and

$$\delta = \frac{1}{2}\ \log\left[\frac{1}{(1-\beta_1)}\ \log\Big(\frac{1}{\beta_1}\Big)\ \left(1+\sqrt{1-\frac{(1-\beta_1)}{\log(\frac{1}{\beta_1})}}\right)^2\right]. \tag{15}$$

The above results differs with the original AJMS calculation [17] where the $\mathcal{F}(\delta)$ term is given by

$$\begin{aligned}
\mathcal{F}(\delta) &= 2\delta - \frac{1}{2}\log\left(\frac{1+\frac{M^2}{s}\ e^{2\delta}}{1+\frac{M^2}{s}e^{-2\delta}}\right) - \frac{\frac{M^2}{s}\cosh(\delta)}{1+2\ \frac{M^2}{s}\ \cosh(\delta)+\frac{M^4}{s^2}}, \\
\delta &= \frac{1}{2}\log\left[\frac{1}{(1-\beta_1)}\ \ \log\Big(\frac{1}{\beta_1}\Big)\ \left(1+\sqrt{1-\frac{(1-\beta_1)^{\frac{1}{2}}}{[\log(\frac{1}{\beta_1})]^{\frac{1}{2}}}}\right)^2\right]\ . \qquad (16)
\end{aligned}$$

5. Model For QGP Evolution

To estimate the energy loss suffered by the heavy quark, it is crucial to calculate its path length which it travel in the medium. Let us assume that the heavy quark is produced at a point $(r,\, \phi)$ in heavy ion collision, moves at an angle ϕ with respect to $\hat{\mathrm{r}}$ in the transverse plane. If R is the radius of the colliding nuclei, then the distance d covered by the heavy quark in the plasma is given [27] by

$$d(\phi,\, r) = \sqrt{R^2 \,-\, r^2 \sin^2\phi} \,-\, r\cos\phi \quad . \tag{17}$$

The average distance travelled by the heavy quark in the plasma

$$L = \frac{\int_0^R \int_0^{2\pi} d(\phi, r)\; \rho(|\vec{r}|)\; \rho(|\vec{r} - \vec{b}|)\; r\; dr\; d\phi}{\int_0^R \int_0^{2\pi} \rho(|\vec{r}|)\; \rho(|\vec{r} - \vec{b}|)\; r\; dr\; d\phi} \quad . \tag{18}$$

Here $\rho(|\vec{r}|)$ is the density of nucleus assumed to be a sharp sphere with radius $R = 1.1\; A^{1/3}$. If the velocity of the heavy quark is $v_T = p_T/m_T$, where m_T is the transverse mass, the effective path length L_{eff} is obtained as

$$L_{eff} = \min\Big[L,\; v_T \;\times\; \tau_f\Big]. \tag{19}$$

The evolution of the system for each centrality bin is governed by an isentropic cylindrical expansion with prescription given in Ref. [28]. The entropy conservation condition $s(T)\, V(\tau) = s(T_0)\, V(\tau_0)$ and equation of state obtained by Lattice QCD along with hadronic resonance are used to obtain temperature as a function of proper time [29]. The transverse size R for a given centrality with number of participant N_{part} is obtained as $R(N_{\rm part}) = R_A\; \sqrt{2\; A/N_{\rm part}}$, where R_A is radius of the nucleus. The initial entropy density $s(\tau_0)$ is

$$s(\tau_0) = \frac{a_{\rm m}}{V(\tau_0)} \left(\frac{dN}{d\eta}\right). \tag{20}$$

Here $a_m = 5$ is a constant which relates the total entropy with the multiplicity [30]. The initial volume $V(\tau_0) = \pi\, [R(N_{\rm part})]^2\, \tau_0$ and measured values of $dN/d\eta$ for LHC [31] and for RHIC [32] are used for a given centrality.

Table 1: Parameters of QGP evolution model

Model	Present	Present	Present	Model [16, 17]	Model [16, 17]
Centrality (%)	0-10	0-100	0-20	0-10	0-20
Experiment	RHIC	LHC	LHC	RHIC	LHC
b (fm)	3.26	9.72	4.70	0.0	0.0
$N_{\rm part}$	329	113	308	-	-
$dN/d\eta$	623	360	1206	-	-
L(fm)	5.63	4.3	5.62	5.78	6.14
τ_0(fm/c)	0.6	0.3	0.3	0.2	0.2
τ_f(fm/c)	3.0	6.0	6.0	2.63	5.90
T_0(GeV)	0.303	0.450	0.481	0.400	0.525

We calculate the energy loss which is then averaged over the temperature evolution. Various parameters used and calculated in our model for different centralities such as number of participant $N_{\rm part}$, measured $dN/d\eta$, calculated average path length (L), initial time (τ_0), QGP life time (τ_f) and initial temperature (T_0) are given in Table 1. The parameters used in the earlier model [16, 17] are also given.

6. Results and Discussions

Figure 4 shows energy loss of charm quark as a function of energy of quark for AuAu collision at $\sqrt{s_{NN}}$=200 GeV using PP, DGLV, AJMS and corrected AJMS formalisms. Figure 5 is the same for bottom quark. It can be seen that the collisional energy loss is similar in magnitude for charm and bottom quark. The radiative energy loss calculated by AJMS is larger than that by DGLV. This difference is more pronounced for bottom quark. Radiative energy loss of bottom quark by AJMS starts dominating collisional energy loss at quark energy above 11 GeV whereas the DGLV energy loss remains below collisional energy loss upto 25 GeV of bottom quark energy. Figure 6 shows energy loss of charm quark as a function of energy of quark for PbPb collision at $\sqrt{s_{NN}}$=2.76

TeV using PP, DGLV, AJMS and corrected AJMS formalisms. Figure 7 is the same for bottom quark. When we move from RHIC to LHC both the collisional as well as radiative energy loss increase. The radiative energy loss of charm quark calculated by AJMS and DGLV are similar in magnitudes but the DGLV energy loss increases more steeply with quark energy. For bottom quark, the AJMS energy loss is much larger than the DGLV energy loss. Radiative energy loss of bottom quark by AJMS starts dominating collisional energy loss at quark energy above 10 GeV whereas the DGLV energy loss remains below collisional energy loss upto 22 GeV of bottom quark energy.

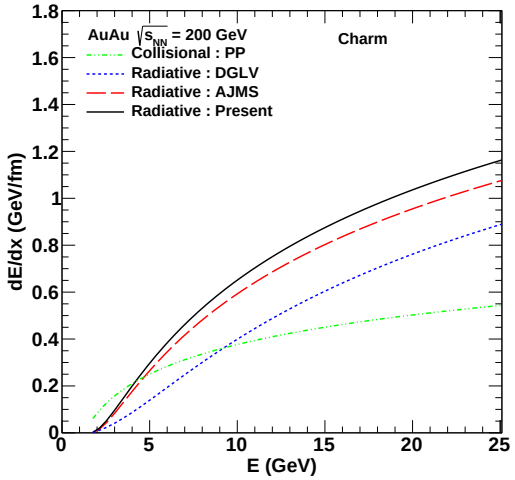


Figure 4: (color online): The energy loss dE/dx as a function of energy of charm quark obtained using PP, DGLV, AJMS and corrected AJMS (Present) calculations for AuAu collision at $\sqrt{s_{NN}}$=200 GeV.

Figure 8 shows nuclear modification factor R_{AA} of single electrons from D meson as a function of transverse momentum p_T obtained using energy loss (DGLV, AJMS, corrected AJMS and DGLV+PP calculations) and shadowing in AuAu collision at $\sqrt{s_{NN}}$=200 GeV. The data is PHENIX measurements of heavy flavour (HF) electrons [23]. We observe that radiative energy loss by DGLV added to collisional energy loss by PP describes the PHENIX data at high

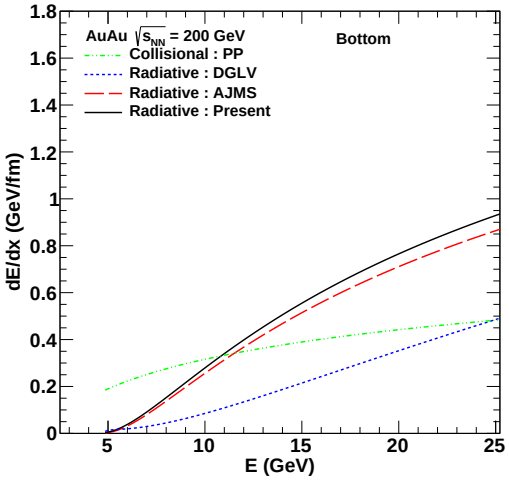


Figure 5: (color online): The energy loss dE/dx as a function of energy of bottom quark obtained using PP, DGLV, AJMS and corrected AJMS (Present) calculations for AuAu collision at $\sqrt{s_{NN}}$=200 GeV.

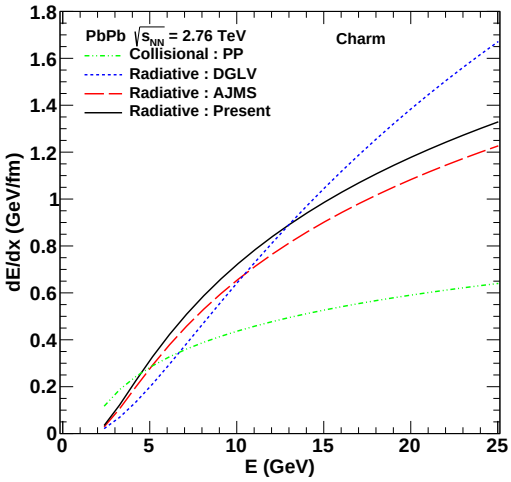


Figure 6: (color online): The energy loss dE/dx as a function of energy of charm quark obtained using PP, DGLV, AJMS and corrected AJMS (Present) calculations for PbPb collision at $\sqrt{s_{NN}}$=2.76 TeV.

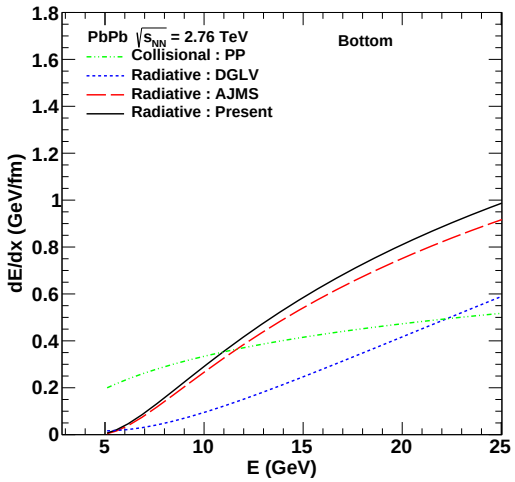


Figure 7: (color online): The energy loss dE/dx as a function of energy of bottom quark obtained using PP, DGLV, AJMS and corrected AJMS (Present) calculations in PbPb collision at $\sqrt{s_{NN}}$=2.76 TeV.

p_T range. The radiative energy loss by AJMS and corrected AJMS reproduce the data without adding energy loss due to collisions.

Figure 9 shows the nuclear modification factor R_{AA} of D meson as a function of transverse momentum p_T obtained using energy loss energy loss (DGLV, AJMS, corrected AJMS and DGLV+PP calculations) and shadowing in AuAu collision at $\sqrt{s_{NN}}$=200 GeV. The data is STAR measurements of D^0 mesons [33]. We observe that the radiative energy loss by AJMS and corrected AJMS reproduce the data without adding energy loss due to collisions. The radiative energy loss by DGLV added to collisional energy loss by PP describes the STAR data at high p_T range.

Figure 10 shows the nuclear modification factor R_{AA} of D^0 mesons as a function of transverse momentum obtained using radiative energy loss (corrected AJMS calculations) calculated with old and new evolution models and shadowing in PbPb collision at $\sqrt{s_{NN}}$= 2.76 TeV. The data is ALICE measurements of D^0 mesons [34] The value of R_{AA} depends on energy loss model as

well as evolution model used to calculate the pathlength.

Figure 11 shows the nuclear modification factor R_{AA} of D^0 mesons as a function of transverse momentum p_T obtained using energy loss (DGLV, AJMS, corrected AJMS and PP+DGLV calculations) and shadowing in PbPb collision at $\sqrt{s_{NN}}$= 2.76 TeV. The data is ALICE measurements of D^0 mesons [34]. AJMS , corrected AJMS and DGLV calculations produce similar suppression in high p_T range. When we add radiative and collisional energy loss (PP+DGLV) it overestimates the measured suppression of D meson.

Figure 12 shows the nuclear modification factor R_{AA} inclusive J/ψ coming from B mesons as a function of transverse momentum p_T obtained using energy loss (DGLV, AJMS, corrected AJMS and PP+DGLV calculations) and shadowing in PbPb collision at $\sqrt{s_{NN}}$= 2.76 TeV. The data is CMS measurements of J/ψ mesons from B decays [35]. We observe that sum of radiative energy loss (DGLV) and collisions energy loss (PP) underestimates the B meson suppression. The sum of radiative energy loss by corrected AJMS and collisions energy loss slightly overestimates the suppression. More accurate data in larger p_T range would help distinguish the models more clearly.

Figure 13 shows the nuclear modification factor R_{AA} of single electrons from D meson as a function of the number of participant N_{part} obtained using energy loss (DGLV, AJMS, corrected AJMS (Present) and PP+DGLV calculations) and shadowing in AuAu collision at $\sqrt{s_{NN}}$=200 GeV compared with the PHENIX measurements of heavy flavour (HF) electrons [23]. The radiative energy loss by DGLV added to collisional energy loss by PP slightly overestimates the suppression. The radiative energy loss by corrected AJMS describes the data without adding energy loss due to collisions.

Figure 14 shows the nuclear modification factor R_{AA} of single electrons from D meson as a function of the number of participant N_{part} obtained using energy loss (DGLV, AJMS, corrected AJMS and PP+DGLV calculations) and shadowing in AuAu collision at $\sqrt{s_{NN}}$ = 200 GeV compared with the STAR measurements of D mesons [33]. We observe that the radiative energy loss by AJMS and corrected AJMS describe the data without adding energy loss due

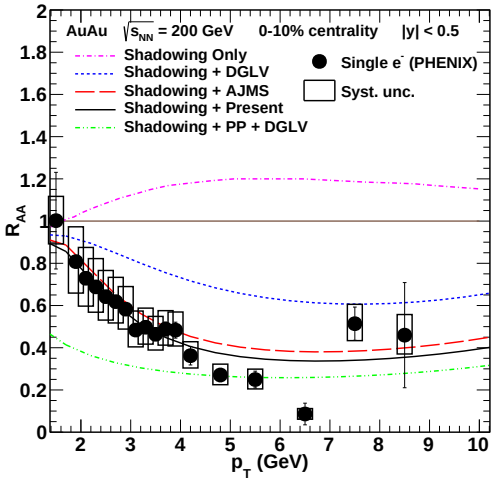


Figure 8: (color online): Nuclear modification factor R_{AA} of single electrons from D meson as a function of transverse momentum p_T obtained using energy loss (DGLV, AJMS, corrected AJMS (Present) and DGLV+PP calculations) and shadowing in AuAu collision at $\sqrt{s_{NN}}$=200 GeV. The data is from PHENIX measurements of heavy flavour (HF) electrons [23].

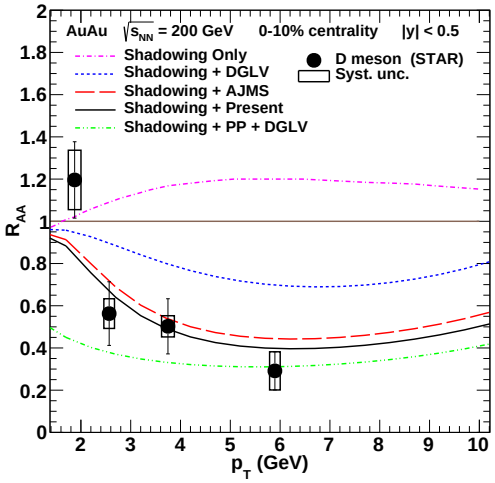


Figure 9: (color online): Nuclear modification factor R_{AA} of D meson as a function of transverse momentum p_T obtained using energy loss (DGLV, AJMS, corrected AJMS (Present) and DGLV+PP calculations) and shadowing in AuAu collision at $\sqrt{s_{NN}}$=200 GeV. The data is from STAR measurements of D mesons [33].

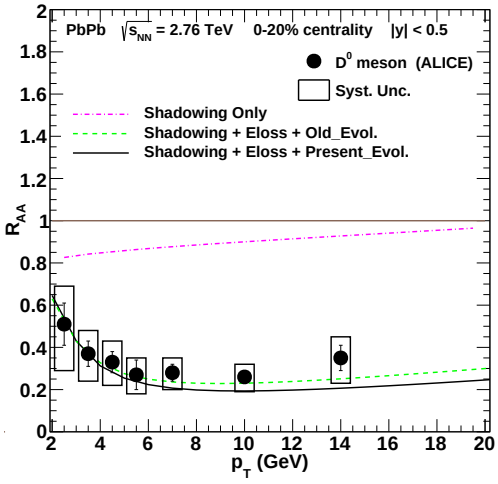


Figure 10: (color online): Nuclear modification factor R_{AA} of D^0 mesons as a function of transverse momentum obtained using radiative energy loss (corrected AJMS (Present) calculations) calculated with old and new evolution models and shadowing in PbPb collision at $\sqrt{s_{NN}}$= 2.76 TeV. The data is from ALICE measurements of D^0 mesons [34].

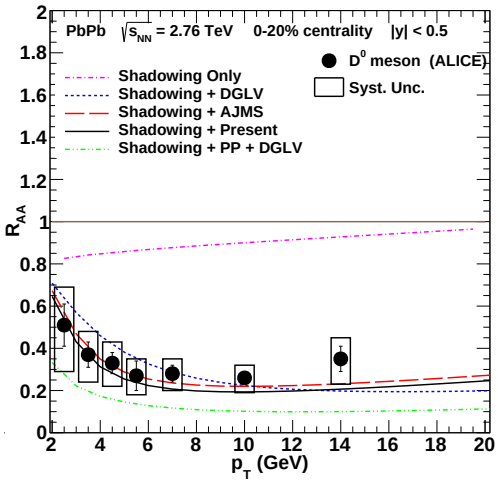


Figure 11: (color online): Nuclear modification factor R_{AA} of D^0 mesons as a function of transverse momentum p_T obtained using energy loss (DGLV, AJMS, corrected AJMS (Present) and PP+DGLV calculations) and shadowing in PbPb collision at $\sqrt{s_{NN}}$= 2.76 TeV. The data is from ALICE measurements of D^0 mesons [34].

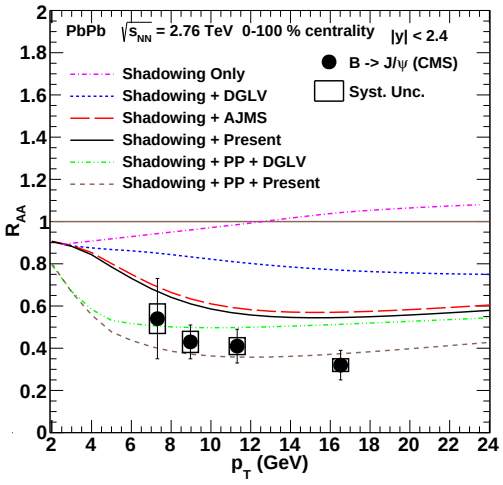


Figure 12: (color online): Nuclear modification factor R_{AA} inclusive J/ψ coming from B mesons as a function of transverse momentum p_T obtained using energy loss (DGLV, AJMS, corrected AJMS (Present) and PP+DGLV calculations) and shadowing in PbPb collision at $\sqrt{s_{NN}}$= 2.76 TeV. The data is from CMS measurements of J/ψ mesons from B decays [35].

to collisions. The energy loss by DGLV does not describe the data.

Figure 15 shows the the nuclear modification factor R_{AA} of D^0 mesons as a function of the number of participant N_{part} obtained using energy loss (DGLV, AJMS, corrected AJMS (Present) and PP+DGLV calculations) and shadowing in the PbPb collision at $\sqrt{s_{NN}}$=2.76 TeV compared with ALICE measurements of D^0 mesons [34]. We observe that the radiative energy loss by DGLV, AJMS and corrected AJMS describe the ALICE data. The radiative energy loss by DGLV added to collisional energy loss by PP overestimates the D^0 suppression.

Figure 16 shows the nuclear modification factor R_{AA} of inclusive J/ψ coming from B mesons as a function of the number of participant N_{part} obtained using energy loss (DGLV, AJMS, corrected AJMS (Present), PP+DGLV and PP+corrected AJMS calculations) and shadowing in the PbPb collision at $\sqrt{s_{NN}}$= 2.76 TeV compared with the CMS measurements of J/ψ mesons from B decays [35]. We observe that the radiative energy loss by DGLV added to

collisional energy loss by PP describes the CMS data very well. The radiative energy loss by corrected AJMS underestimates the suppression but with collisional energy loss added it overestimates the suppression. Both the models favour that B meson loose energy by radiation as well as collision processes.

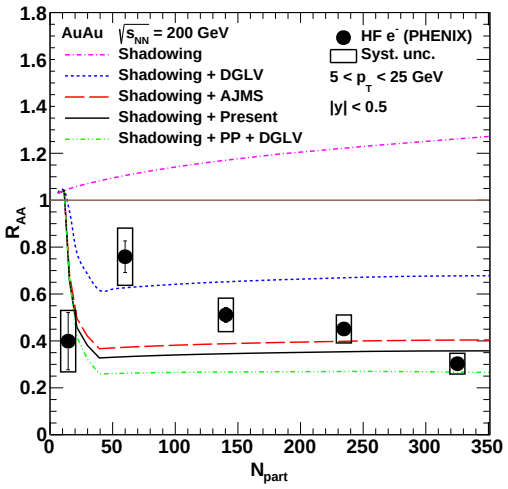


Figure 13: (color online): Nuclear modification factor R_{AA} of single electrons from D meson as a function of the number of participant N_{part} obtained using energy loss (DGLV, AJMS, corrected AJMS (Present) and PP+DGLV calculations) and shadowing in AuAu collision at $\sqrt{s_{NN}}$=200 GeV. The data is from PHENIX measurements of heavy flavour (HF) electrons [23].

7. Conclusion

We study the energy loss of heavy quark (charm and bottom) due to elastic collisions and gluon radiation in hot/dense medium. Results of Radiative energy loss obtained from two different formalisms namely DGLV and AJMS have been compared. The energy loss calculated by AJMS exceeds DGLV results. The collisional energy loss has been calculated using Peigne and Peshier formalism and is found to be similar in magnitude for charm and bottom quarks. The nuclear modification factors R_{AA} including shadowing and energy loss are evaluated for

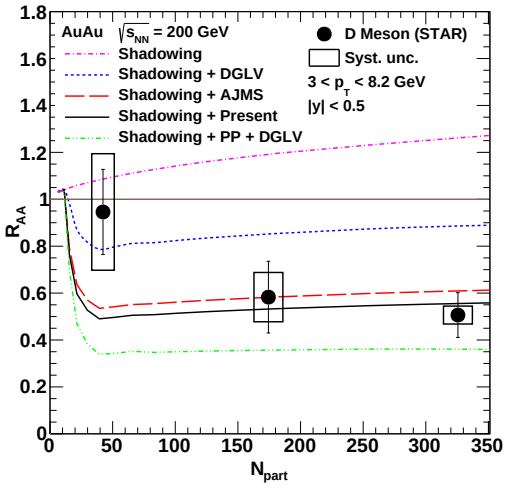


Figure 14: (color online): Nuclear modification factor R_{AA} of single electrons from D meson as a function of the number of participant N_{part} obtained using energy loss (DGLV, AJMS, corrected AJMS (Present) and PP+DGLV calculations) and shadowing in AuAu collision at $\sqrt{s_{NN}}$=200 GeV. The data is from STAR measurements of D mesons [33].

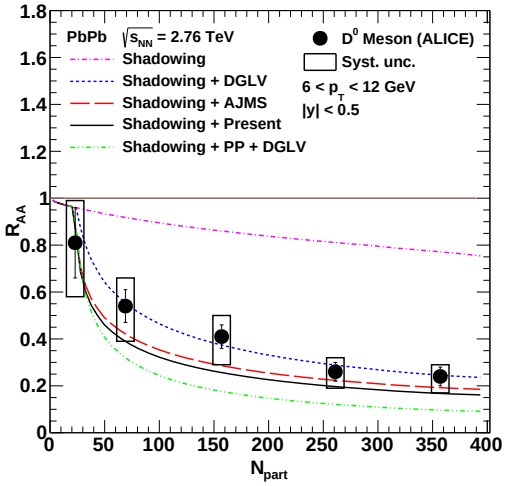


Figure 15: (color online): Nuclear modification factor R_{AA} of D^0 mesons as a function of the number of participant N_{part} obtained using energy loss (DGLV, AJMS, corrected AJMS (Present) and PP+DGLV calculations) and shadowing in the PbPb collision at $\sqrt{s_{NN}}$=2.76 TeV. The data is from ALICE measurements of D^0 mesons [34].

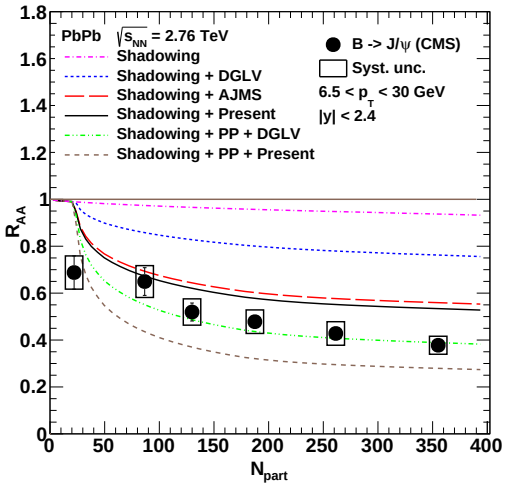


Figure 16: (color online): Nuclear modification factor R_{AA} of inclusive $J\psi$ coming from B mesons as a function of the number of participant N_{part} obtained using energy loss (DGLV, AJMS, corrected AJMS (Present), PP+DGLV and PP+corrected AJMS calculations) and shadowing in the PbPb collision at $\sqrt{s_{NN}}$= 2.76 TeV. The data is from CMS measurements of J/ψ mesons from B decays [35].

B and D mesons and are compared with the measurements in PbPb collision at $\sqrt{s_{NN}} = 2.76$ TeV and with the HF electrons and D^0 meson measurements in AuAu collision at $\sqrt{s_{NN}} = 200$ GeV. The radiative plus collisional energy loss (PP+DGLV) describes the RHIC HF electron suppression in high p_T range. It also describes the LHC measurement of B meson suppression but overestimates the suppression of D meson. The radiative energy loss from generalized dead cone approach describes the charm suppression at both RHIC as well as LHC energies without requiring collisional energy loss. Both collision as well as radiative energy loss are required to explain the B meson suppression at LHC. Upcoming high luminosity PbPb collisions at $\sqrt{s_{NN}} = 5$ TeV are expected to measure the heavy quarks in wider kinematic ranges which will provide much improved constrains for the processes of energy loss and models.

Acknowledgements

We are thankful to Umme Jamil, M. G. Mustafa , D. K. Shrivastava and V. Kumar for many fruitful discussions.

Appendix A: DGLV Formalism

The average radiative energy loss of heavy quarks as

$$\frac{\Delta E}{L} = E\,\frac{C_F\alpha_s}{\pi}\frac{1}{\lambda}\int_{\frac{m_g}{E+p}}^{1-\frac{M}{E+p}} dx \int_0^\infty \frac{4\,\mu_g^2\,q^3\,dq}{\left(\frac{4Ex}{L}\right)^2+(q^2+\beta^2)^2}\times(A\log B+C) \quad (21)$$

where

$$\beta^2 = m_g^2(1-x)+M^2x^2,\quad \lambda^{-1}=\rho_g\sigma_{Qg}+\rho_q\sigma_{Qq}\ , \quad (22)$$

$$\rho_g = 16\,T^3\,\frac{1.202}{\pi^2},\quad \rho_q = 9\,N_f\,T^3\,\frac{1.202}{\pi^2}, \quad (23)$$

$$\sigma_{Qq} = \frac{9\pi\alpha_s^2}{2\mu_g^2} \text{ and } \sigma_{Qg}=\frac{4}{9}\sigma_{Qq}\ . \quad (24)$$

Here $C_F(=4/3)$ determines the coupling strength of gluon to the massive quark with momentum p. ρ_g and ρ_q are the densities of gluons and quarks and $m_g = \mu_g/\sqrt{2}$ is the transverse gluon mass.

The function A, B and C are given as follows

$$A = \frac{2\beta^2}{f_\beta^3}\left(\beta^2+q^2\right), \tag{25}$$

$$B = \frac{(\beta^2+K)(\beta^2 Q_\mu^- + Q_\mu^+ Q_\mu^+ + Q_\mu^+ f_\beta)}{\beta^2\Big(\beta^2(Q_\mu^- - K) - Q_\mu^- K + Q_\mu^+ Q_\mu^+ + f_\beta f_\mu\Big)}, \tag{26}$$

$$\begin{aligned} C = {} & \frac{1}{2q^2 f_\beta^2 f_\mu}\left[\beta^2\mu_g^2(2q^2-\mu_g^2) + \beta^2(\beta^2-\mu_g^2)K\right. \\ & + Q_\mu^+(\beta^4 - 2q^2 Q_\mu^+) + f_\mu\Big(\beta^2(-\beta^2 - 3q^2 + \mu_g^2) \\ & \left. + 2q^2 Q_\mu^+\Big) + 3\beta^2 q^2 Q_k^-\right]. \end{aligned} \tag{27}$$

Here

$$K = k_{max}^2 = 2px(1-x), \tag{28}$$

$$Q_\mu^\pm = q^2 \pm \mu_g^2, \quad Q_k^\pm = q^2 \pm k_{max}^2, \tag{29}$$

$$f_\beta = f(\beta, Q_\mu^-, Q_\mu^+), \quad f_\mu = f(\mu_g, Q_k^+, Q_k^-), \tag{30}$$

$$f(x,y,z) = \sqrt{x^4 + 2x^2 y + z^2}. \tag{31}$$

Appendix B: Corrected AJMS

The integration of Eq. (12) are obtained as follows.

The minimum values of $q_\perp^2$, ω and $k_\perp^2$ are given by infra-red cut-off [17, 25, 36, 37]

$$q_\perp^2|_{min} \approx \omega_{min}^2 \approx k_\perp^2|_{min} \approx \mu_g^2. \tag{32}$$

The maximum value of $q_\perp^2|_{max}$ is calculated as [36, 37, 38]

$$q_\perp^2|_{max} = C\ E\ T\ , \tag{33}$$

where

$$C = \frac{3}{2} - \frac{M^2}{4\ E\ T} + \frac{M^4}{48\ E^2\ T^2\ \beta_0}\ \log\Big[\frac{M^2 + 6\ E\ T\ (1+\beta_0)}{M^2 + 6\ E\ T\ (1-\beta_0)}\Big] \tag{34}$$

and

$$\beta_0 = \sqrt{1 - \frac{M^2}{E^2}}\ . \tag{35}$$

The maximum value of ω is obtained as [39]

$$\omega_{max}^2 =< q_\perp^2 > \ . \tag{36}$$

The average of square of the transverse momentum $q_\perp$ is given in reference [36, 37] as

$$< q_\perp^2 >= \frac{q_\perp^2|_{min}\ q_\perp^2|_{max}}{q_\perp^2|_{max} - q_\perp^2|_{min}}\ \log\Big[\frac{q_\perp^2|_{max}}{q_\perp^2|_{min}}\Big]\ . \tag{37}$$

Putting $q_\perp^2|_{min}$ from Eq. (32) and $q_\perp^2|_{max}$ from Eq. (33) in Eq. (37)

$$< q_\perp^2 >= \frac{\mu_g^2}{(1-\beta_1)}\ \log\Big[\frac{1}{\beta_1}\Big], \tag{38}$$

where $\beta_1 = \ \mu_g^2/(C\ E\ T)$. Using the relation $\omega = k_\perp\ \cosh\eta$, the finite cut on ω and $k_\perp$ leads to an inequality

$$\frac{\omega_{max}}{k_\perp|_{min}}\ <\ \cosh\eta. \tag{39}$$

The integration limits of η are calculated from Eq. (32), (36) and (39) as

$$|\eta| < \log\left(\sqrt{\frac{< q_\perp^2 >}{\mu_g^2}} + \sqrt{\frac{< q_\perp^2 >}{\mu_g^2} - 1}\right). \tag{40}$$

We can write it as $|\eta| < \delta$, where δ is obtained using equation (38) and (40)

$$\delta = \frac{1}{2}\ \log\left[\frac{1}{(1-\beta_1)}\ \log\Big(\frac{1}{\beta_1}\Big)\ \left(1 + \sqrt{1 - \frac{(1-\beta_1)}{\log(\frac{1}{\beta_1})}}\right)^2\right]. \tag{41}$$

We can write the minimum and maximum value of η as

$$\eta_{min} = -\delta, \quad \eta_{max} = \delta. \tag{42}$$

Now we calculate the integrals in Eq. (12) which can be written as

$$\frac{dE}{dx} = 24\ \alpha_s^3\ \rho_{QGP}\ I_1\ I_2\ I_3\ \ . \tag{43}$$

The first integration I_1 is calculated as

$$I_1 = \int_{\mu_g^2}^{C\ E\ T} \frac{1}{(q_\perp^2)^2}\ dq_\perp^2 = \frac{1}{\mu_g^2}\ \Big(1 - \beta_1\Big). \tag{44}$$

The second integration I_2 is calculated as

$$I_2 = \int_{\omega_{\min}}^{\omega_{max}} d\omega = \mu_g \left(\sqrt{\frac{1}{(1-\beta_1)} \log\left(\frac{1}{\beta_1}\right)} - 1 \right). \tag{45}$$

The third integration I_3 is calculated as

$$I_3 = \int_{\eta_{min}}^{\eta_{max}} \mathcal{D}\, d\eta = \int_{-\delta}^{\delta} \frac{1}{\left(1 + \frac{M^2}{s}\, e^{2\eta}\right)^2}\, d\eta \ , \tag{46}$$

$$= \frac{1}{2} \left[\frac{1}{1 + \frac{M^2}{s}\, e^{2\eta}} + \log\left(\frac{\frac{M^2}{s}\, e^{2\eta}}{1 + \frac{M^2}{s}\, e^{2\eta}} \right) \right]_{-\delta}^{\delta} \ , \tag{47}$$

$$= \frac{1}{2} \left[\log(e^{4\delta}) + \log\left(\frac{1 + \frac{M^2}{s}\, e^{-2\delta}}{1 + \frac{M^2}{s}\, e^{2\delta}} \right) - \left(\frac{\frac{M^2}{s}\, (e^{2\delta} - e^{-2\delta})}{1 + \frac{M^2}{s}\, (e^{2\delta} + e^{-2\delta}) + \frac{M^4}{s^2}} \right) \right] \tag{48}$$

The integration I_3 is denoted as $\mathcal{F}(\delta)$ given by

$$\mathcal{F}(\delta) = 2\delta - \frac{1}{2} \log\left(\frac{1 + \frac{M^2}{s}\, e^{2\delta}}{1 + \frac{M^2}{s}\, e^{-2\delta}} \right) - \left(\frac{\frac{M^2}{s}\, \sinh(2\delta)}{1 + 2\, \frac{M^2}{s} \cosh(2\delta) + \frac{M^4}{s^2}} \right) \ . \tag{49}$$

References

References

[1] Quark Matter 2014, Nucl. Phys. A**931** (2014) 1-1266.

[2] V. Kumar, P. Shukla and R. Vogt, Phys. Rev. C**86** (2012) 054907 [arXiv:1205.3860 [hep-ph]].

[3] J. D. Bjorken, Fermilab preprint Pub-**82/59**-THY (1982).

[4] E. Braaten and M. H. Thoma,Phys. Rev. D**44** (1991) 1298.

[5] E. Braaten and M. H. Thoma, Phys. Rev. D**44** (1991) 2625.

[6] A. Peshier, Phys. Rev. Lett. **97** (2006) 212301 [hep-ph/0605294].

[7] S. Peigne and A. Peshier, Phys. Rev. D**77** (2008) 114017 [arXiv:0802.4364 [hep-ph]].

[8] N. Armesto, C. A. Salgado and U. A. Wiedemann, Phys. Rev. D**69** (2004) 114003 [hep-ph/0312106];

[9] N. Armesto, C. A. Salgado and U. A. Wiedemann, Phys. Rev. C**72** (2005) 064910 [hep-ph/0411341].

[10] M. Gyulassy, P. Levai and I. Vitev, Phys. Rev. Lett. **85** (2000) 5535 [nucl-th/0005032].

[11] M. Djordjevic and M. Gyulassy, Nucl. Phys. A**733** (2004) 265 [nucl-th/0310076].

[12] U. Jamil and D. K. Srivastava, J. Phys. G**37** (2010) 085106 [arXiv:1005.1208 [nucl-th]].

[13] M. B. Gay Ducati, V. P. Goncalves and L. F. Mackedanz, hep-ph/0506241.

[14] M. Gyulassy, P. Levai and I. Vitev, Nucl. Phys. B**571** (2000) 197 [hep-ph/9907461].

[15] M. Gyulassy, P. Levai and I. Vitev, Nucl. Phys. B**594** (2001) 371 [nucl-th/0006010].

[16] S. Wicks, W. Horowitz, M. Djordjevic and M. Gyulassy, Nucl. Phys. A**784** (2007) 426 [nucl-th/0512076].

[17] R. Abir, U. Jamil, M. G. Mustafa and D. K. Srivastava, Phys. Lett. B**715** (2012) 183 [arXiv:1203.5221 [hep-ph]].

[18] H. L. Lai, M. Guzzi, J. Huston, Z. Li, P. M. Nadolsky, J. Pumplin and C.-P. Yuan, Phys. Rev. D**82**, (2010) 074024 [arXiv:1007.2241 [hep-ph]].

[19] R. E. Nelson, R. Vogt and A. D. Frawley, Phys. Rev. C**87**,(2013) 014908 [arXiv:1210.4610 [hep-ph]].

[20] K. J. Eskola, H. Paukkunen and C. A. Salgado, JHEP **0904** (2009) 065 [arXiv:0902.4154 [hep-ph]].

[21] C. Peterson, D. Schlatter, I. Schmitt and P. M. Zerwas, Phys. Rev. D**27** (1983) 105.

[22] T. Sjostrand, S. Mrenna and P. Z. Skands, JHEP **0605**,(2006) 026 [hep-ph/0603175].

[23] A. Adare *et al.* [PHENIX Collaboration], Phys. Rev. C**84** (2011) 044905 [arXiv:1005.1627 [nucl-ex]].

[24] B. Abelev *et al.* [ALICE Collaboration], JHEP **1207**, (2012) 191 [arXiv:1205.4007 [hep-ex]].

[25] R. Abir, C. Greiner, M. Martinez, M. G. Mustafa and J. Uphoff, Phys. Rev. D**85** (2012) 054012 [arXiv:1109.5539 [hep-ph]].

[26] T. S. Biro, E. van Doorn, B. Muller, M. H. Thoma and X. N. Wang, Phys. Rev. C**48**(1993) 1275 [nucl-th/9303004]

[27] B. Muller, Phys. Rev. C**67** (2003) 061901 [nucl-th/0208038].

[28] X. Zhao and R. Rapp, Nucl. Phys. A**859** (2011) 114.

[29] V. Kumar and P. Shukla, arXiv:1410.3299 [hep-ph].

[30] E. V. Shuryak, Phys. Rev. Lett. **68** (1992) 3270.

[31] K. Aamodt *et al.* [ALICE Collaboration], Phys. Rev. Lett. **106** (2011) 032301 [arXiv:1012.1657 [nucl-ex]].

[32] B. B. Back *et al.* [PHOBOS Collaboration], Phys. Rev. C**65** (2002) 061901 [nucl-ex/0201005].

[33] L. Adamczyk *et al.* [STAR Collaboration], Phys. Rev. Lett. **113**, (2014) 142301 [arXiv:1404.6185 [nucl-ex]].

[34] B. Abelev *et al.* [ALICE Collaboration], JHEP **1209** (2012) 112 [arXiv:1203.2160 [nucl-ex]].

[35] CMS Collaboration [CMS Collaboration], CMS-PAS-HIN-12-014.

[36] M. G. Mustafa, D. Pal, D. K. Srivastava and M. Thoma, Phys. Lett. B**428** (1998) 234 [nucl-th/9711059].

[37] W. C. Xiang, H. T. Ding and D. C. Zhou, Chin. Phys. Lett. **22** (2005) 72.

[38] M. G. Mustafa, D. Pal, D. K. Srivastava and M. Thoma, Phys. Lett. B**428** (1998) 234 [nucl-th/9711059].

[39] X. N. Wang, M. Gyulassy and M. Plumer, Phys. Rev. D**51**, (1995) 3436 [hep-ph/9408344].